

Two-Stage, Global-Local Approach for Cell Nuclei Segmentation in Histopathology Images

Amit Shakya Revat Saharan Chetan Gupta Rupesh Kumar Lalit Sharma
Srivatsava Naidu Subrahmanyam Murala Chetan Arora

This paper, titled “Two Stage, Global-Local Approach for Cell Nuclei Segmentation in Histopathology Image,” was published in the proceedings of CVIP-2024 and is available via IEEE Xplore (DOI: 10.1109/CVIP57892.2024.10899523).

Reprinted with permission. Copyright © 2024 IEEE.
Further use or distribution is not permitted without permission from IEEE.

Abstract

Effective management of high-resolution, and spatially wide contextual cues is fundamental to the accurate semantic segmentation. Traditional approaches like multi-resolution feature maps, and skip-connection are effective but require changes in the backbone architecture, restricting utilization of newer models and architectures for the problem. In this work we propose an architecture-agnostic, two-stage, global-local framework, called GoLo, for the semantic segmentation, which can use arbitrary semantic segmentation models within its two stages. We focus on segmenting cell nuclei in histopathology image analysis, where accurate segmentation of cell nuclei boundaries is one of the key issues. The proposed framework consists of first stage with Global and second stage with Local learning approach. The first stage is proposed to process the image globally and provide the coarse nuclei segmentation map. In the second stage, to process the image locally, coarse segmentation map and input image is first converted into patches. These patches are then fed as input to the second stage to get the fine-grained segmentation map. Both stages are trained with a combination of dice and binary cross entropy loss. To show the effectiveness of our approach, we test 4 state-of-the-art segmentation architectures (ACC-UNet, UCTransnet, Swin-UNet, and Vanilla U-Net), on 4 different benchmark datasets (MoNuSeg, CPM-17, CoNSep, and TNBC). We evaluate performance of each technique before and after using our framework. We report an average improvement of 4.82% in mIoU, and 4.52% mDSC score, across techniques, and datasets.

1 INTRODUCTION

A. Background

Cancer ranks as the second leading cause of death and disease burden worldwide, following cardiovascular disease^[1]. It emphasizes the critical need for early detection to improve treatment outcomes. Changes in the shape and structure of cell nuclei are significant indicators in cancer diagnosis. Histopathological examination is the primary method in which pathologists diagnose cancer by visually inspecting tissue changes and cellular abnormalities under a microscope. This process is time-consuming and highly reliable on human expertise^[2]. Studies have shown significant variability among pathologists in diagnosing biopsies, with an average disagreement rate of 24.7%^[3]. This high

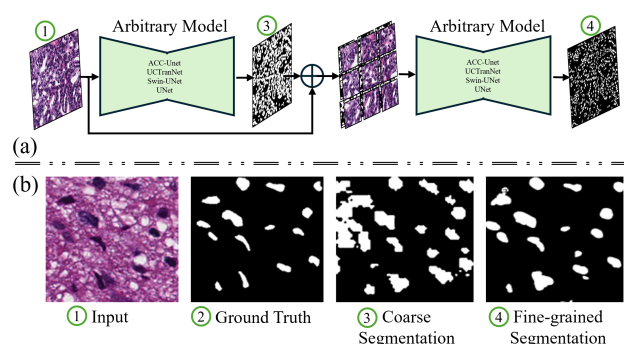


Fig. 1 The key idea of this work is to use a two-stage framework for accurate segmentation. In the first stage, we use the full image (which needs to be inputted at a lower resolution due to memory constraints) with a state-of-the-art model (we have experimented with ACC-UNet, UCTranNet, Swin-UNet, and U-Net), which identifies all the nuclei but with inaccurate boundaries (image 3). In the second stage, we crop each individual nuclei based on the mask in the first stage (along with a small context around the boundary), and give full resolution version which leads to accurate boundaries (image 4)

variability highlights the potential for computer-assisted histopathology interpretation to improve diagnostic consistency and accuracy.

B. Cell Nuclei Segmentation

One of the most important and fundamental task for computer-assisted histopathology interpretation is cell nuclei segmentation. It refers to the process of identifying and delineating the boundaries of cell nuclei within images obtained from microscopy. In traditional approaches to cell nuclei segmentation, scientists employed techniques such as Water- shed segmentation, K-means clustering, and fuzzy C-means to delineate cell nuclei within histopathology images^[4]. These methods have limited performance for blurry images. So, scientists are looking for better ways to do this job automatically and accurately^[5]. Deep learning has emerged as a superior solution for cell nuclei segmentation due to its ability to automatically learn and extract features from images, leading to more accurate and robust segmentation results^[6]. Unlike traditional methods, deep learning models can segment nuclei of different cells with diverse image conditions^{[7][8]}. This adaptability is crucial in biomedical imaging, where nuclei can vary greatly in size, shape, and intensity. Once trained, deep learning models can process large-scale image datasets quickly, making them suitable for high-throughput analysis. While these methods have shown some performance gains, they still suffer from issues like complex post processing and excessive redundant computations. While traditional methods have been effective to some extent, they often require manual intervention and parameter tuning, leading to subjective results and limited generalizability. U-Net^[9], an architecture built on Fully Convolutional Networks (FCN), is widely used and has achieved excellent results in medical image segmentation. Many single stage approaches have been proposed, an extensive review is presented in [10].

C. Two-Stage Approaches for Cell Nuclei Segmentation

Among the numerous studies aimed at improving the original U-Net^{[11]-[13]} there has been considerable focus on stacking or cascading multiple U-Nets. Sevastopolsky et

al.^[13] combine two types of building blocks, U-Net and Res- U-Net, to segment images of the optic disc and cup image segmentation. Christ et al.^[12] use a sequential arrangement of two U-Nets to segment both the liver and lesions in CT images. In [14], an ensemble of FCN-based methods was introduced to distinguish overlapped segmented nuclei. Although this approach achieved better results than basic encoder-decoder models, it struggled with more difficult cases^[15]. We observe that existing methods are often dependent on specific architectures. For example, Jiang et al.^[16] proposed a two-step approach using a modified U-Net model: initially, a simplified U-Net variant generates a preliminary prediction, and then, in the second step, the architecture is enhanced by adding two decoding layers to refine the prediction. In contrast, our approach is architecture-agnostic. It allows the use of any arbitrary architecture in both the global and local stages, providing flexibility and refinement for cell nuclei segmentation without being tied to a specific model structure.

D. Our Proposal

The key trade-off for an accurate segmentation is managing resolution and context. While per-pixel predictions can give a high-resolution mask, clearly delineating the boundaries, the context at individual pixel is often not enough to label. Giving context from a patch helps predict the label accurately but sacrifices the resolution. Our key observation is that the current two-stage state-of-the-art techniques which give binary segmented mask in the first stage do provide the necessary context, but by providing the full image in the second stage, doesn't allow the model to focus on high resolution which is crucial for accurate boundary segmentation. Hence, in this work, we propose a simple, yet highly effective technique which does coarse level segmentation in the first stage by using the full image. However, in the second stage, we crop the images according to the mask generated in the first stage, and then give high resolution images to the network in the second stage for highly accurate boundary prediction. Figure 1 visually describes our approach. Our main contributions are:

- We propose a novel two stage global-local learning approach for cell nuclei segmentation which effectively combines contextual cues with high resolution features for accurate boundary segmentation.
- The proposed pipeline is architecture agnostic, and can combine multiple latest evolving segmentation techniques in the two stages.
- Our proposed framework outperforms existing state-of-the-art techniques on four publicly available datasets.

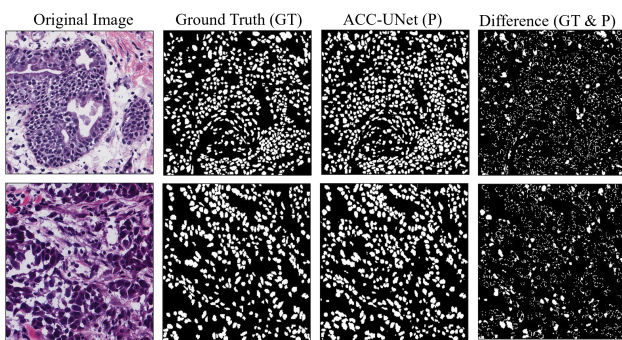


Fig. 2 Limitations in Nuclei Boundary Segmentation: Implications for Disease Diagnosis

2 PROPOSED APPROACH

Nuclei segmentation is important in medical imaging because it helps to clearly identify and outline the nuclei of cells in complicated tissue images. Several methods are used for nuclei segmentation^{[4]-[6][10]} and while they effectively locate nuclei, they often struggle with precisely defining their boundaries (see Figure 2). This limitation raises concerns about their overall effectiveness. To address this critical aspect of biomedical image processing there is a dire need of refinement. In this work, we argue that providing localized features, along with the entire image can enhance the boundary delineation. The architecture of our proposed approach is illustrated in Figure 3. In this study, we propose a novel approach to nuclei segmentation using a two-stage learning framework called Global-Local (GoLo). The first stage is Global, and the second stage is Local. In a two-stage learning framework, we use the same segmentation model twice in sequence, with the second stage refining the results of the first one. The pipeline is designed such that the input image fed into the model and the resulting

segmented binary mask are of same original size.

In Stage-1 (Global), a U-Net based model is employed to globally process the histopathological images, aiming to predict the coarse binary segmentation map. To train this model, a combination of binary cross entropy and dice loss functions is utilized, facilitating the optimization process by penalizing deviations between the predicted and ground truth segmentation masks. However, this stage excels in accurately localizing nuclei, but have limitations with accurately delineating fine boundaries. To address this, the resulting segmentation mask from Stage-1 is resized to match the original image size ($N \times N$) and then concatenate it with the input image. This process creates a four-channels image, incorporating both the original input image and the predicted segmentation mask of Stage-1. The four channel image consist of localization information into the input from Stage-1, enhancing the model's ability to capture spatial relationships between nuclei and their surroundings. Subsequently, this four-channel image is cropped into patches of size 100×100 , serving as preprocessing for the Stage-2 model. In Stage-2 (Local), the same U-Net based model is employed, receiving the cropped patches of four-channel images as input. With the localization of cell nuclei already provided from first stage output as one of the channels in input, the primary focus of this model is to precisely delineate the boundaries of nuclei. Leveraging the rich spatial context encoded in the four channels, the model works to refine the segmentation by capturing fine details and accurately delineating boundaries. The predicted segmentation masks, resized back to 100×100 patches, are then stitched together to reconstruct the full segmented image (see Figure 3). This stitching process ensures that the model effectively integrates information from multiple patches to produce a final binary segmented mask with smoother and more accurate boundaries. This refined segmentation is essential for enabling precise diagnosis and analysis in medical imaging applications. Final binary segmentation map is obtained by stitching together all the patches generated by the second stage. Formally, let's define some terms:

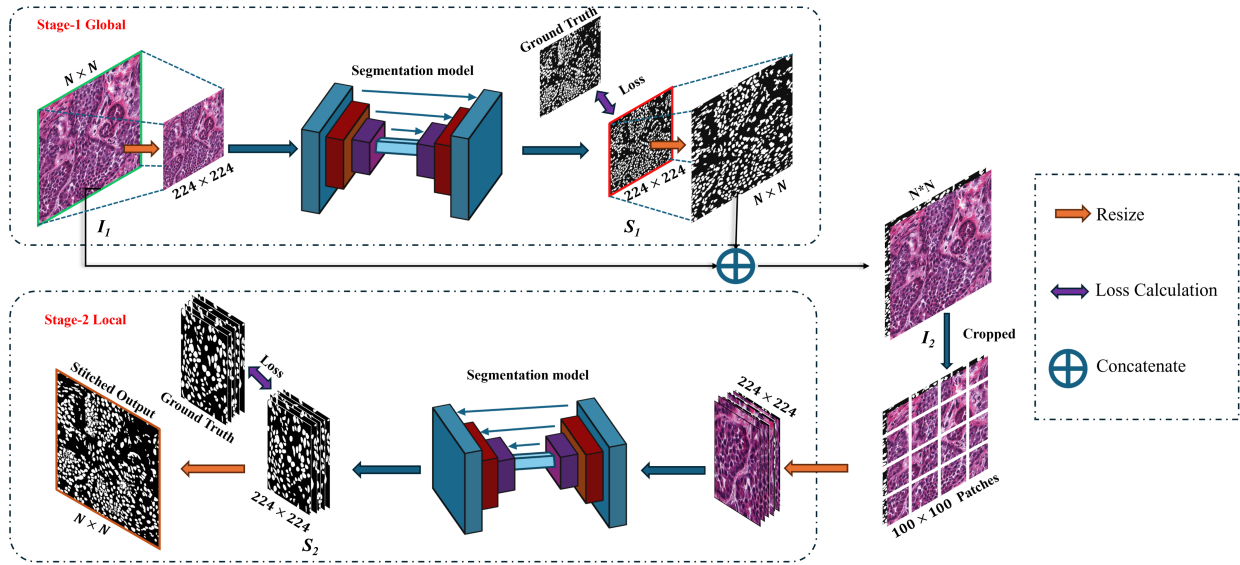


Fig. 3 Proposed Approach: Two Stages, Global- local features extractions (GoLo)

Table 1 COMPARATIVE QUANTITATIVE RESULTS FOR CELL NUCLEI SEGMENTATION

Datasets		MoNuSeg		CPM-17		CoNSeP		TNBC	
Methods	Approach	mDSC	mIoU	mDSC	mIoU	mDSC	mIoU	mDSC	mIoU
UNet	Existing	69.81	55.12	83.55	72.00	74.21	59.18	70.77	54.35
	Proposed	74.11	60.67	87.05	77.23	77.31	63.14	74.08	59.39
Swin-UNet	Existing	65.58	49.81	79.08	69.60	61.00	41.23	66.75	50.35
	Proposed	73.79	60.17	85.08	74.23	76.91	62.64	72.61	57.27
UCTransnet	Existing	74.30	60.07	85.67	75.18	67.86	51.68	75.28	60.66
	Proposed	77.38	63.80	86.85	76.94	74.58	59.68	74.67	59.85
ACC-UNet	Existing	75.04	62.41	83.94	72.54	74.03	58.92	73.35	58.18
	Proposed	77.93	65.93	86.87	76.97	75.69	61.01	77.74	57.51

- I_1 represents an input image. In our case, it belongs to the RGB image domain, denoted as $I_1 \in R^{w \times h \times 3}$, where w and h represent the width and height of the image, respectively.
- S_1 denotes the binary segmentation map obtained from the first stage. It belongs to a set of possible segmentation maps $S_1 \in \{0, 1\}^{224 \times 224 \times 1}$. It is resized to $w \times h \times 1$
- $I_2 \in R^{w \times h \times 4}$ which is the channel-wise concatenation of resized S_1 and I_1 both of size $w \times h$. It is then cropped into patches of 100×100 .
- S_2 represents the binary segmentation map generated from the Stage 2. It belongs to a set of binary maps $\in \{0, 1\}^{224 \times 224 \times 1}$ which again resized to 100×100 . These patches are then stitched together to form the final binary segmentation map belongs to a set $\{0, 1\}^{w \times h \times 1}$

This stage takes the original image I_1 as input to UNet based model^{[9][17]-[19]}, generating a binary segmentation map S_1 , which highlights the locations of the nuclei ignoring the fine boundaries. 2. Second Stage (Local): This stage uses the patches of I_2 as input to U-Net based model, the output segmentation maps are stitched together to create the full binary segmentation map. The stitched segmented map has more accurate nuclei boundaries.

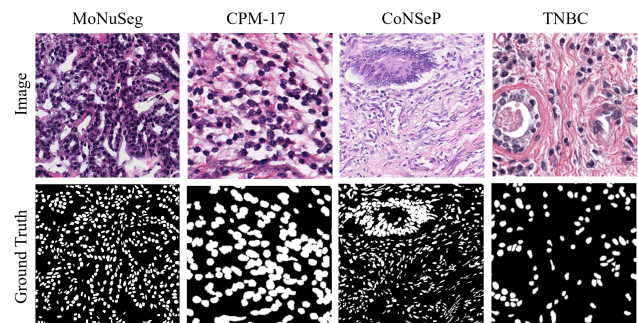


Fig. 4 Samples from different datasets

In the two-stage learning framework: 1. First Stage (Global):

A. Data Processing and Network Training

1) *Datasets Description*: To assess the effectiveness of the Global-Local training approach, we carried out experiments using four publicly available datasets: Multi-Organ Nucleus Segmentation^[17], CPM-17^[20], Colorectal Nucleus Segmentation and Phenotype^[21], and Triple Negative Breast Cancer Dataset^[22] each targeting different types of cell nuclei. *Multi-organ Nuclei Segmentation (MoNuSeg)*^[17] dataset contains 44 image tiles, each sized $1,000 \times 1,000$ pixels. It contains Whole Slide Images (WSIs) of 7 organs (breast, kidney, colon, stomach, prostate, liver, and bladder) from various medical centres (i.e., various stains) of high-resolution WSI of H&E-stained slides from nine tissue types, digitised at $40 \times$ magnification in eighteen different hospitals and obtained from National Cancer Institute's cancer Genome Atlas (TCGA). *CPM-17*^[20] dataset consists of 32 images obtained from the University Hospitals Coventry and Warwickshire (UHCW). These images were captured using magnifications of $40 \times$ and $20 \times$, with sizes ranging from 500×500 to 600×600 pixels. Within this dataset, a total of 7,570 nuclei have been meticulously annotated and labeled. It offers tissue images with annotated labels for nuclei segmentation and classification, sourced from patients diagnosed with head and neck squamous cell carcinoma (HNSCC), glioblastoma multiforme (GBM), non-small cell lung cancer (NSCLC), and lower-grade glioma (LGG) tumors. These nuclei span across four distinct cancer types, providing a diverse set of cellular structures for analysis and segmentation purposes. The *CoNSeP* dataset^[21] contains 41 image tiles, each sized 1000×1000 pixels, obtained from colorectal adenocarcinoma (CRA) WSIs. These images were scanned at $40 \times$ objective magnification using an Omnyx VL120 scanner at the pathology department of University Hospitals Coventry and Warwickshire, UK. Naylor et al.^[22] introduced a dataset called *Triple Negative Breast Cancer (TNBC)*. The dataset consists of 50 H&E-stained images, each with a resolution of 512×512 pixels, and includes a total of 4022 annotated nuclei. These images are extracted from histopathological samples of 11 patients diagnosed with triple-negative breast cancer. Dataset includes various cell types such as normal epithelial and myoepithelial

breast cells, invasive carcinomatous cells, fibroblasts, endothelial cells, adipocytes, macrophages, and inflammatory cells, providing a comprehensive representation of the histological features observed in TNBC samples. To train the network on these datasets we utilized random flip and rotation augmentation.

2) *Training Loss*: The proposed approach is dedicated to semantic segmentation, and its loss function is constructed using both Binary Cross-Entropy (BCE) loss and Dice loss. These two are commonly used loss functions in biomedical image segmentation. BCE evaluates class predictions for each pixel individually, while Dice loss quantifies the overlap between two samples. To optimize performance and achieve early convergence in our task, we utilize a BCE-Dice loss function, which combines binary cross-entropy with Dice loss, resulting in improved performance and faster convergence. We formally define the loss function as Overall loss, L_O

$$L_O = 0.5L_{BCE} + 0.5L_{DICE} \quad (1)$$

$$L_{BCE} = - \left[\frac{1}{n} \sum_{i=1}^{N \times K} X_i \log Y_i + \sum_{i=1}^{N \times K} (1 - X_i) \log (1 - Y_i) \right] \quad (2)$$

$$L_{DICE} = 1 - \frac{2 \sum_{i=1}^{N \times K} X_i Y_i + \epsilon}{\sum_{i=1}^{N \times K} Y_i + \sum_{i=1}^{N \times K} X_i + \epsilon} \quad (3)$$

Within equation 2 and 3, X_i represent the ground truth mask and Y_i represent the segmented mask. n denotes total number of nuclear pixels within the image and $N \times K$ denotes the set containing all pixels.

3 RESULTS AND DISCUSSION

The proposed approach is quantitatively compared with existing approaches (UNet^[9], Swin-Unet^[23], UCTransnet^[19], and ACC-UNet^[18]) in terms of mean Dice Similarity Coefficient (mDSC) and mean Intersection over Union (mIoU) on the MoNuSeg, CPM-17, CoNSeP, and TNBC datasets. Notably, our approach demonstrates superior mean DSC and mean (IoU) metrics, in comparison to

baseline methods indicating its effectiveness for nuclei segmentation tasks (see Table I). To ensure a fair comparison, we adhered to the same training and testing

set split criteria as employed for the baseline methods. Furthermore, in Figure 5 we provide visual comparisons

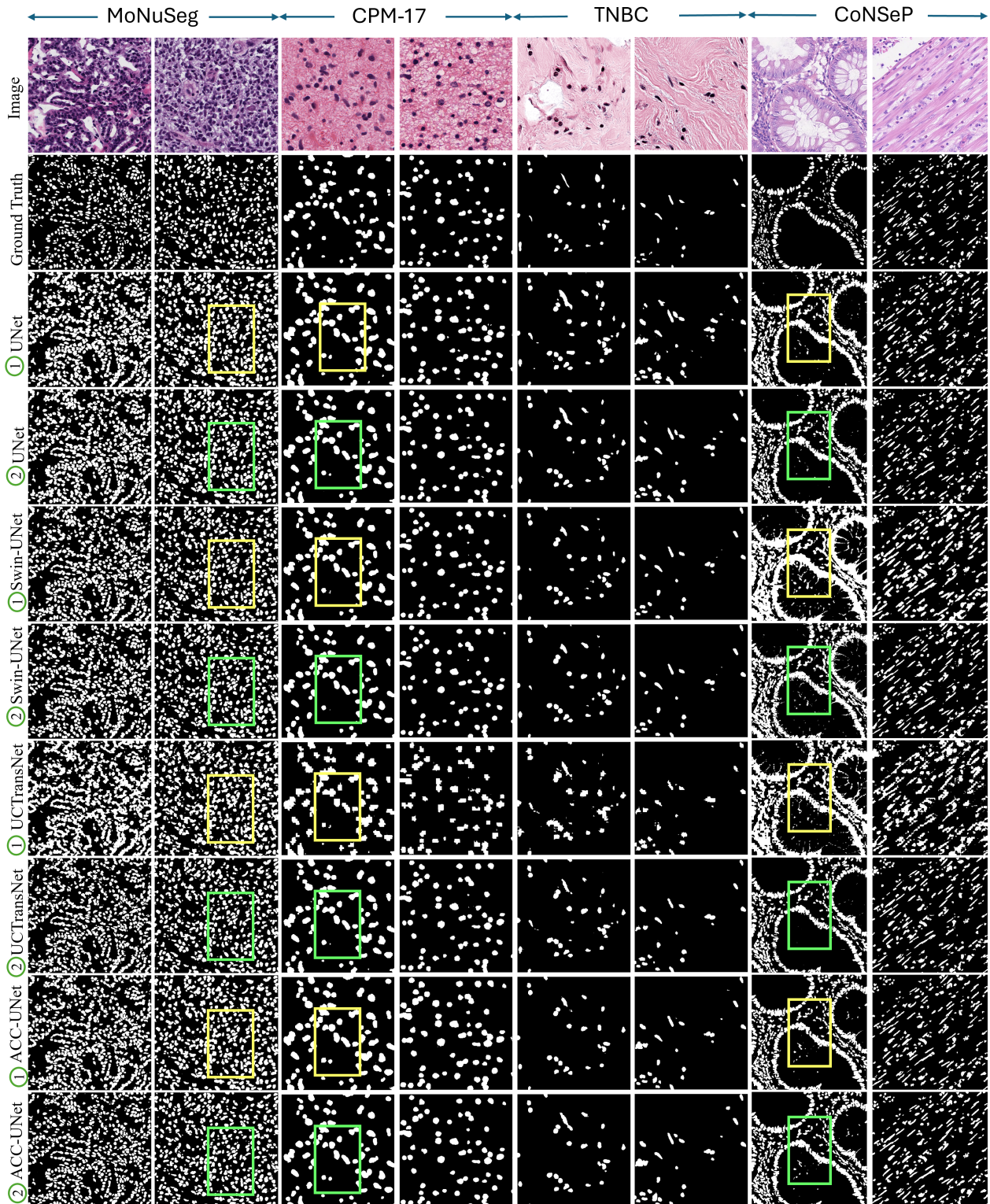


Fig. 5 Comparative results of nuclei segmentation on MoNuSeg, CPM-17, TNBC and CoNSEP dataset. Input image with their corresponding ground truth along with the segmentation results of existing methods (single-stage ①) and Proposed approach (GoLo ②)

between the segmentation results of our approach and the existing methods for MoNuSeg, CPM-17, CoNSeP, and TNBC datasets. For the MoNuSeg dataset, our approach refine the boundaries in comparison to existing methods (see box in Figure 5). Figure 5 show results on CoNSeP dataset, our prediction filtered out the apparent nodule region, which was predicted as a false positive by all the other models (see green box which signify the improvement in comparison to yellow box). In the CPM-17 and TNBC dataset, we not only successfully predicted the localization of nuclei but also identified fine boundaries that were mostly missed by the existing models. As clearly depicted in Figure 5 our Global-Local approach effectively delineates nuclei boundaries, outperforming the baseline models. Overall, our proposed model achieves state-of-the-art accuracy in nuclei segmentation by leveraging auxiliary information. This approach holds promise for direct deployment in cell pathology diagnosis systems, aiming to alleviate the workload of pathologists. It is important to note that our approach demonstrates a high level of generalization across varying tissue and cell types.

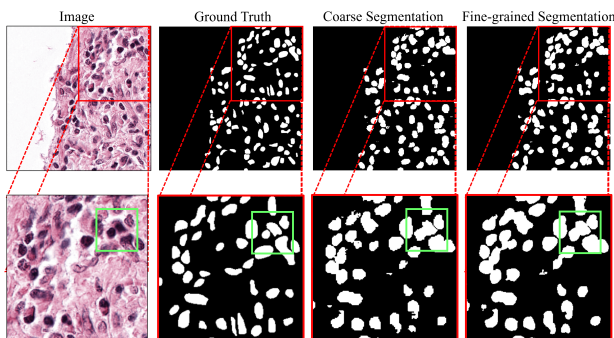


Fig. 6 Limitation of our proposed approach

A. Limitations of Proposed Approach

Though the proposed architecture offers significant benefits towards boundary delineation of nuclei, it performs poorly for touching nuclei with the unclear or blurred boundary (see the bounding box in the cropped portion of Figure 6). A traditional approach to address the touching cell nuclei problem involves applying a distance transform to the segmentation mask, followed by using a watershed algorithm. Although this method often proves ineffective for highly overlapping cases, this

observation will be considered as the future scope to further improve the segmentation accuracy of proposed approach.

4 CONCLUSION

In this study, we propose a novel two-stage learning approach called GoLo for cell nuclei segmentation in histopathology images, representing a significant advancement in addressing the nuclei boundary segmentation challenge. Breaking down the segmentation process into two distinct steps allows us to leverage global features for preliminary nucleus localization and boundary detection, followed by the refinement of boundaries using local features and additional information obtained in the first stage. In the end, our concept is architecture agnostic, universal which can be readily applicable to various histopathology image analysis applications.

REFERENCES

- [1] H. Wang, M. Naghavi, C. Allen, R. M. Barber, Z. A. Bhutta, A. Carter, D. C. Casey, F. J. Charlson, A. Z. Chen, M. M. Coates et al., "Global, regional, and national life expectancy, all-cause mortality, and cause-specific mortality for 249 causes of death, 1980-2015: a systematic analysis for the global burden of disease study 2015," *The Lancet*, vol. 388, pp. 1459-544, 2016.
- [2] W. He, T. Liu, Y. Han, W. Ming, J. Du, Y. Liu, Y. Yang et al., "A review: The detection of cancer cells in histopathology based on machine vision," *Computers in Biology and Medicine*, vol. 146, p. 105636, 2022.
- [3] W. Hsu, S. X. Han, C. W. Arnold, A. A. Bui, and D. R. Enzmann, "A data-driven approach for quality assessment of radiologic interpretations," *Journal of the American Medical Informatics Association*, vol. 23, no. e1, pp. e152-e156, 2016.
- [4] R. M. Thomas and J. John, "Detection and segmentation of mitotic cell nuclei in breast histopathology images," in *2017 International Conference on Networks & Advances in Computational Technologies (NetACT)*. IEEE, 2017, pp. 246-250.

- [5] A. Das, M. S. Nair, and S. D. Peter, "Computer-aided histopathological image analysis techniques for automated nuclear atypia scoring of breast cancer: a review," *Journal of digital imaging*, vol. 33, no. 5, pp. 1091-1121, 2020.
- [6] T. Wan, L. Zhao, H. Feng, D. Li, C. Tong, and Z. Qin, "Robust nuclei segmentation in histopathology using asppu-net and boundary refinement," *Neurocomputing*, vol. 408, pp. 144-156, 2020.
- [7] N. Kumar, R. Verma, S. Sharma, S. Bhargava, A. Vahadane, and A. Sethi, "A dataset and a technique for generalized nuclear segmentation for computational pathology," *IEEE Transactions on Medical Imaging*, vol. 36, no. 7, pp. 1550-1560, 2017.
- [8] P. Naylor, M. Laé, F. Reyat, and T. Walter, "Segmentation of nuclei in histopathology images by deep regression of the distance map," *IEEE Transactions on Medical Imaging*, vol. 38, no. 2, pp. 448-459, 2019.
- [9] O. Ronneberger, P. Fischer, and T. Brox, "U-net: Convolutional networks for biomedical image segmentation," in *Medical image computing and computer-assisted intervention—MICCAI 2015: 18th international conference*, vol. 18, 2015, pp. 234-241.
- [10] F. Xing and L. Yang, "Robust nucleus/cell detection and segmentation in digital pathology and microscopy images: a comprehensive review," *IEEE Reviews in Biomedical Engineering*, vol. 9, pp. 234-263, 2016.
- [11] L. Bi and et al., "Dermoscopic image segmentation via multistage fully convolutional networks," *IEEE Transactions on Biomedical Engineering*, vol. 64, no. 9, pp. 2065-2074, 2017.
- [12] P. Christ and et al., "Automatic liver and lesion segmentation in ct using cascaded fully convolutional neural networks and 3d conditional random fields," in *MICCAI*. Springer, 2016, pp. 415-423.
- [13] A. Sevastopolsky and et al., "Stack-u-net: Refinement network for image segmentation on the example of optic disc and cup," *arXiv preprint arXiv:1804.11294*, 2018.
- [14] P. Naylor, M. Laé, F. Reyat, and T. Walter, "Nuclei segmentation in histopathology images using deep neural networks," in *14th IEEE International Symposium on Biomedical Imaging*, 2017, pp. 933-936.
- [15] —, "Segmentation of nuclei in histopathology images by deep regression of the distance map," *IEEE Transactions on Medical Imaging*, vol. 38, no. 2, pp. 448-459, 2019.
- [16] Z. Jiang, C. Ding, M. Liu, and D. Tao, "Two-stage cascaded u-net: 1st place solution to brats challenge 2019 segmentation task," in *International MICCAI Brainlesion Workshop*, 2019, pp. 231-241.
- [17] N. Kumar, R. Verma, D. Anand, Y. Zhou, O. F. Onder, E. Tsougenis, H. Chen, P.-A. Heng, J. Li, Z. Hu et al., "A multi-organ nucleus segmentation challenge," *IEEE transactions on medical imaging*, vol. 39, no. 5, pp. 1380-1391, 2019.
- [18] N. Ibtehaz and D. Kihara, "Acc-unet: A completely convolutional unet model for the 2020s," in *International Conference on Medical Image Computing and Computer-Assisted Intervention*. Springer Nature Switzerland, 2023, pp. 692-702.
- [19] H. Wang, P. Cao, J. Wang, and O. R. Zaiane, "Uctransnet: rethinking the skip connections in u-net from a channel-wise perspective with transformer," in *Proceedings of the AAAI conference on artificial intelligence*, vol. 36, no. 3, 2022, pp. 2441-2449.
- [20] Q. Vu, S. Graham, T. Kurc, M. To, M. Shaban, T. Qaiser, N. Koohbanani, S. Khurram, J. Kalpathy-Cramer, T. Zhao, R. Gupta, J. Kwak, N. Rajpoot, J. Saltz, and K. Farahani, "Methods for segmentation and classification of digital microscopy tissue images," *Frontiers in Bioengineering and Biotechnology*, vol. 7, p. 53, 2019. [Online]. Available: <https://doi.org/10.3389/fbioe.2019.00053>
- [21] S. Graham, Q. Vu, S. Raza, A. Azam, Y. Tsang, J. Kwak, and N. Rajpoot, "Hover-net: simultaneous segmentation and classification of nuclei in multi-tissue histology images," *Medical Image Analysis*, vol. 58, p. 101563, 2019. [Online]. Available: <https://doi.org/10.1016/j.media.2019.101563>
- [22] P. Naylor, M. Laé, F. Reyat, and T. Walter, "Segmentation of nuclei in histopathology images by deep regression of the distance map," *IEEE Transactions on Medical Imaging*, vol. 38, pp. 448-459, 2019. [Online]. Available: <https://doi.org/10.1109/TMI.2018.2865709>
- [23] H. Cao, Y. Wang, J. Chen, D. Jiang, X. Zhang, Q. Tian, and M. Wang, "Swin-unet: Unet-like pure transformer for medical image segmentation," in *European conference on computer vision*. Springer, 2022, pp. 205-218.

■ 著者



Amit Shakya
Emerging Technology and
Innovation Lab,
Yamaha Motor Solutions India
Department of Biomedical
Engineering, Indian Institute
of Technology Ropar, India



Revat Saharan
Emerging Technology and
Innovation Lab,
Yamaha Motor Solutions India



Chetan Gupta
Emerging Technology and
Innovation Lab,
Yamaha Motor Solutions India



Rupesh Kumar
Emerging Technology and
Innovation Lab,
Yamaha Motor Solutions India



Lalit Sharma
Emerging Technology and
Innovation Lab,
Yamaha Motor Solutions India



Srivatsava Naidu
Department of Biomedical
Engineering, Indian Institute
of Technology Ropar, India



Subrahmanyam Murala
School of Computer Science
and Statistics, Trinity College
Dublin, Ireland



Chetan Arora
Department of Computer
Science and Engineering,
Indian Institute of Technology
Delhi, India